International Journal of Research
Available at https://edupediapublications.org/journals
e-ISSN: 2348-6848
p-ISSN: 2348-795X
Volume 05 Issue-01
January 2018

Stress Distribution around Polygonal Holes in Graphite/Epoxy Laminates Under in Plane Loading

[1]A.Rohith, [2]Dr.A.Raveendra,[3]Dr.D.K.Nageswara Rao,[4]M.Ramesh Babu

[1] Pg Scholar, Department Of Mech, Mallareddy Engineering College, Maisammaguda, Dulapally Road, Hyderabad, T S India

[2]Associate Professor, Department Of Mech, Mallareddy Engineering College, Maisammaguda, Dulapally Road, Hyderabad, T S India

[3]Hod, Department Of Mech, Mallareddy College Of Engineering And Technology, Maisammaguda, Dulapally Road, Hyderabad, T S India

[4]Associate Proessor, Department Of Mech, Vaagdevi College Of Engineering, Warangal, T S India

Abstract:

An analytical solution is presented to determine the stress distribution around polygonal holes in symmetric Graphite/epoxy laminates under inplane loading. Basic formulation given by Savin has been adopted and enhanced by introducing into it the generalized mapping function and arbitrary biaxial loading condition. These features have provided extra dimension to consider any shape of hole and any kind of inplane loading. The validity of the solution is cheeked by reproducing the results of various authors in the literature. This solutions is extremely useful to study the effect of hole shape, type of loading, fiber orientation, laminate geometry and stacking sequence on stress distribution. These parameters are studied for symmetric laminates containing different shapes of holes and loading conditions. The results of the present solutions are satisfactory when compared with the results in the literature. Results obtained from the general solution for inplane loading are also validated by FEM results obtained from ANSYS.

INTRODUCTION

Preliminary Remarks

Fiber reinforced composite laminates find wide applications in aerospace, under-water, automotive and many other weight sensitive structures due to their superior structural properties like, high specific strength, high specific stiffness, more corrosion resistance and more thermal stability, etc., over the conventional materials. Cutouts are made into the laminates for service requirements that result in strength degradation. In order to predict the structural behavior of these laminates with some degree of assurance, it is necessary to study the effect of anisotropy and type of loading on stress distribution around the cutouts.The present work is to derive the solutions for determining the stresses around any shape of hole in symmetric laminates under remotely applied inplane loads.

Composite Materials

The word composite in composite material signifies that two or more materials are combined on a macroscopic scale to form a useful material. In laminated fiber-reinforced composites, layers of reinforced material are built up with the fiber directions of each layer typically oriented in different directions to get different values of strength and stiffness.

A lamina is the basic building block in fiber reinforced composite laminates. A lamina or ply is a plane or curved layer of unidirectional fibers or woven fabric in a matrix. It is also referred to as unidirectional lamina,

which is an orthotropic material in its principal directions. A lamina is made up of two or more unidirectional laminae or plies stacked together at various orientations. The configuration of the laminate indicating its ply composition is called lay-up. The configuration indicating, in addition to the ply composition, the exact location or sequence of various plies is called the stacking sequence.

A symmetric laminate will have an identical lamina at a particular distance on either side of the mid-plane. These laminates find wide applications because of their simplicity in construction and ease of analysis of the laminate. Unsymmetric laminates are those in which no mid-plane symmetry will be present. Antisymmetric cross ply and angle ply laminates are special forms of unsymmetric laminates.

Mechanical Behavior of Composite Materials

In contrast to the more conventional engineering materials, the composite materials are often both heterogeneous and non-isotropic (orthotropic or, more generally, anisotropic).

An orthotropic body has material properties that are different in three mutually perpendicular directions at a point in the body and, further has three mutually perpendicular planes of material symmetry.

An anisotropic body has material properties that are different in all directions at a point in the body and no planes of material property symmetry exist. However, in both orthotropic and anisotropic cases, the properties are a function of orientation at a point in the body.

For orthotropic materials, like isotropic materials, application of normal stress along principal material direction results in extension in the direction of applied stress and contraction in the perpendicular direction to the applied stress. Shear stress causes shearing deformation. Unlike the isotropic materials, the shear modulus is independent of other material properties.

For anisotropic materials, the application of normal stress leads not only to extension in the direction of the stress and contraction perpendicular to it, but also to shearing deformation. Conversely, shearing stress causes extension and contraction in addition to the distortion of shearing deformation. This coupling between both loading modes and both deformation modes, i.e., shear-extension coupling, is also a characteristic of orthotropic materials subjected to normal stress in a non-principal material direction.

Aim and Scope of the Work

The aim of the present work is to obtain an analytical solution to determining the stress distribution around polygonal holes in a laminate with layers of arbitrary fiber orientation and stacking sequence. The solutions obtained shall consider any shape of hole such as circular, elliptical, triangular, square, rectangular and several irregular shaped holes, etc., in symmetric. The solution presented shall consider various cases of inplane loading, viz., uniaxial and biaxial stresses.

LITERATURE REVIEW

Preliminary Remarks

Analytical methods of stress analysis greatly facilitate parametric study and provide benchmarking results. Lekhnitskii [1] and Savin [2] gave the solutions for stresses around holes in anisotropic and isotropic plates using the complex variable method. As on today, the research on stress concentration problems especially in fiber reinforced composite laminates is ongoing.

Solutions for Inplane Loading

Anisotropic Case

Lekhnitskii; the characteristic feature of Lekhnitskii's solutions is the application of series method for determining the stress functions. A general expression of the form

$$x = a\,(\cos\theta + \varepsilon \cos N\theta)$$
$$y = a\,(c\,\sin\theta - \varepsilon \sin N\theta\,)$$

is used to define circular, elliptical, oval, triangular and square holes with rounded corners and curved edges. *a, c,* ε and N are the constants determining the size and shape of the hole. The boundary conditions and stress functions are taken in series form.

Isotropic Case

Gao

In the general solution for infinite elastic isotropic plate with an elliptic hole, Gao has considered various cases of loading through an arbitrary biaxial loading condition. The stresses are applied about an arbitrary coordinate system that has been rotated by an angle $\beta$from another coordinate system coinciding with the principal body directions. The biaxial loading factor λgives the ratio of stress applied along the two coordinate axes in the arbitrary coordinate system. By taking appropriate values of λ and β, several cases of loading are considered in the solution, such as: hydrostatic tension, inclined simple tension, pure shear, cracked plate under biaxial tension, loading case in thin walled pressure vessels.

THEORETICAL FORMULATION

Preliminary Remarks

In the present work, general solutions are presented within the classical laminated plate theory for two-dimensional stresses or moments around holes in thin fiber reinforced composite laminates. The stresses and displacements are considered in terms of complex stress functions. The given hole problem is regarded as superposition of two sub-problems corresponding to a sum of the respective complex potentials. The first sub-problem consists of the loaded laminate without hole ensuring remote boundary conditions. The second sub problem considers the hole, loaded with those tractions that appear as internal forces along the fictitious hole boundary in the first sub problem. Thus the two sub problems together also ensure the boundary conditions along the hole edge.General solutions of inplane and bending loads on symmetric laminates are obtained by introducing the generalized form of mapping function.

Generalized Form of Mapping Function

In the theory of complex variables, conformal mapping facilitates representing the area external to a given hole in z-plane by the area outside the unit circle in ζ-plane using a transformation function called the mapping function. Such a mapping function is given in a generalized form as:

$$z = \omega(\zeta) = R\left(\zeta + \sum_{k=1}^{N} \frac{m_k}{\zeta^k}\right) \quad \text{.....3.1}$$

where, m_k are the constants of the mapping function. The computer program for each of the solutions is developed to consider a maximum number of terms N equal to 1 to 19. More number of terms in the mapping function will be useful in the convergence studies. By introducing the constants m_k for a given shape of hole into the program, the results for corresponding hole can be obtained. R is a constant for size of the hole. In the present analysis, the effect of hole size is not considered and hence R is taken equal to unity and the stress or moment distribution obtained is independent of the hole size.

The mapping function in Eq.(3.1) corresponds to the isotropic case and it is further modified to consider anisotropy. Taking $\zeta = \rho\, e^{i\theta}$,where ρ, θ are the coordinates in ζ-plane and by taking $\rho = 1$ for the unit circle, we have:

$$\zeta = (\cos\theta + i\ \sin\theta) \qquad \text{...(3.2)}$$

Inserting Eq(3.2) into Eq.(3.1), we get

$$z=\omega(\zeta)=R\left[\left(\cos\theta+\sum_{k=1}^{N}m_k\cos k\theta\right)+i\left(\sin\theta-\sum_{k=1}^{N}m_k\sin k\theta\right)\right]$$

...(3.3)

By introducing the complex parameters of anisotropy s_j into Eq.(3.3), by affine transformation, z becomes

$$z_j=\omega_j(\zeta)=R\left[\left(\cos\theta+\sum_{k=1}^{N}m_k\cos k\theta\right)+s_j\left(\sin\theta-\sum_{k=1}^{N}m_k\sin k\theta\right)\right] \quad ...(3.4)$$

The complex quantities s_j in Eq.(3.4) depend on the type of loading, material of the laminate and its geometry. They are determined from the roots of the characteristic equation (3.15) of the biharmonic equation (3.14) for inplane loading. Using the following identities into Eq.(3.4),

$$\cos k\theta = \frac{1}{2}\left(\zeta^k+\frac{1}{\zeta^k}\right), \quad \sin k\theta = \frac{-i}{2}\left(\zeta^k-\frac{1}{\zeta^k}\right) \quad ...(3.5)$$

the mapping function (3.4) takes the final form as:

$$z_j=\omega_j(\zeta) = \frac{R}{2}\left[a_j\left(\frac{1}{\zeta}+\sum_{k=1}^{N}m_k\zeta^k\right)+b_j\left(\zeta+\sum_{k=1}^{N}\frac{m_k}{\zeta^k}\right)\right] \quad ...(3.6)$$

where, $a_j = (1 + i\ s_j)$, $b_j = (1 - i\ s_j)$ $(j=1,\ldots,4)$ …(3.7)

The mapping function zj in Eq. (3.6) will be introduced into the equations of the boundary conditions of the given problem while determining the stress functions.

Arbitrary Biaxial Loading Condition

In order to consider several cases of inplane or bending loads, the arbitrary biaxial loading condition is introduced into the boundary conditions. This condition considers any arbitrary orientation of uniaxial and biaxial stresses or moments as well as, shear stress or twisting moment applied at infinity.

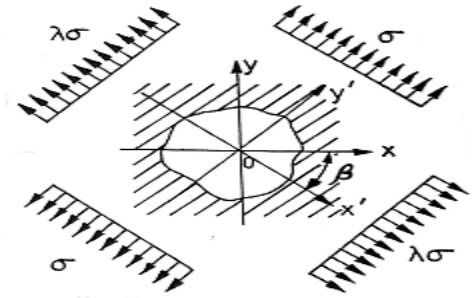

Fig. 3.1 Plate Containing Hole under Arbitrary Biaxial Loading condition

An infinite plate with an arbitrary shape of hole subjected to inplane loading under arbitrary biaxial loading condition is shown in Fig.3.1. This condition has been adapted from Gao's [15] solution for the elliptical hole in isotropic plate. By means of this condition, solutions for biaxial loading or shear stress or twisting moment can be obtained without the need for superposition of the solutions of the uniaxial loading. This is achieved by merely introducing the biaxial loading factor λ and the orientation angle β into the boundary conditions at infinity. A remotely applied loading is considered about the arbitrary coordinate axes $x'0y'$ that make an angle β with $x0y$ axes in the principal directions of the body

Boundary Conditions at Infinity

The boundary conditions about the arbitrary coordinate axes $x'0y'$ for each class of loading are given in the following:

For inplane loading of symmetric laminates:

$$\sigma_x^\infty = \lambda\sigma; \quad \sigma_y^\infty = \sigma; \quad \tau_{x'y'}^\infty = 0 \quad at\ |z|\to\infty \quad ...(3.8)$$

By applying the relation of transformation of axes, the boundary conditions in Eqs.(3.8) about $x0y$ axes are given by :

$$\begin{aligned}\sigma_{x'}^\infty+\sigma_{y'}^\infty &= \sigma_x^\infty+\sigma_y^\infty \\ \sigma_{y'}^\infty-\sigma_{x'}^\infty+2i\,\tau_{x'y'}^\infty &= \left(\sigma_y^\infty-\sigma_x^\infty+2i\,\tau_{xy}^\infty\right)e^{2i\beta}\end{aligned} \quad ...(3.9)$$

International Journal of Research
Available at https://edupediapublications.org/journals
e-ISSN: 2348-6848
p-ISSN: 2348-795X
Volume 05 Issue-01
January 2018

Similarly by applying the relations (3.11) to the boundary conditions Eqs.(3.9) and (3.10) also, the boundary conditions about *x0y* axes can be written explicitly as :

$$\sigma_x^{\infty} = \frac{\sigma}{2}[(\lambda+1)+(\lambda-1)\cos 2\beta]$$
$$\sigma_y^{\infty} = \frac{\sigma}{2}[(\lambda+1)-(\lambda-1)\cos 2\beta] \quad \ldots (3.10)$$
$$\tau_{xy}^{\infty} = \frac{\sigma}{2}[(\lambda-1)\sin 2\beta]$$

The boundary conditions in Eqs.(3.10) will be useful in determining the stress functions of the hole free plate.

Applications of Arbitrary Biaxial Loading Condition

With reference to Fig. 3.1, the following values of λ and β will be taken into Eqs.(3.10) to obtain different conditions of loading.

1. Inclined uniaxial tension or cylindrical bending : $\lambda = 0, \beta \neq 0$
   (a) Loading along *x*-axis : $\lambda = 0, \beta = \pi/2$
   (b) Loading along *y*-axis : $\lambda = 0, \beta = 0$
2. Hydrostatic tension or all-round moment at infinity: $\lambda = 1, \beta \neq 0$
   (a) Equibiaxial tension or moment : $\lambda = 1, \beta = 0$
3. Shear stress or twisting moment : $\lambda = -1, \beta = \pi/4$ or $3\pi/4$

General Solution for Inplane Loading of Symmetric Laminates

Complex Variable Formulation A thin anisotropic plate is considered under generalized plane stress condition. The thickness *h,* is taken in *z*-direction and *x0y* plane is taken as the midplane of the plate. It is assumed that the external forces act on the side surfaces of the plate in such a way that the resultant of these forces for the entire height *h,* is situated in the *x0y* plane. The other surfaces of the plate, namely the 'top' one at $z = +h/2$ and the 'bottom' one at $z = -h/2$ are assumed to be free of external forces, i.e., $\sigma_z = \tau_{yz} = \tau_{xz} = 0$ for $z = \pm h/2$.

The plate is considered to be thin due to the value of h/R being small, where R denotes the size of the hole. The stresses $\sigma_z, \tau_{yz}, \tau_{xz}$ are zero everywhere inside the plate in addition to being zero on top and bottom surfaces of the plate. Due to consideration of generalized plane stress, the mean values of strain or stress components over the thickness are taken into the equations instead of the actual stress components. For the sake of simplicity, these mean values are represented by $\varepsilon_x, \varepsilon_y, \gamma_{xy}, \sigma_x, \sigma_y, \tau_{xy}$ without bars over the symbols. From the generalized Hooke's law, the mean values of strains along the thickness of the plate are given by:

$$\begin{aligned}\varepsilon_x &= a_{11}\sigma_x + a_{12}\sigma_y + a_{16}\tau_{xy}\\ \varepsilon_y &= a_{12}\sigma_x + a_{22}\sigma_y + a_{26}\tau_{xy}\\ \gamma_{xy} &= a_{16}\sigma_x + a_{26}\sigma_y + a_{66}\tau_{xy}\end{aligned} \quad \ldots (3.11)$$

The six elastic constants $a_{11}, a_{22}, a_{12}, a_{66}, a_{16}, a_{26}$ in Eq.(3.11) are defined in Appendix-I

Representing σ_x , σ_y, τ_{xy} in terms of Airy's stress function $U(x,y)$,

$$\sigma_x = \frac{\partial^2 U}{\partial y^2} \quad \sigma_y = \frac{\partial^2 U}{\partial x^2} \quad \tau_{xy} = -\frac{\partial^2 U}{\partial x \partial y} \quad \ldots (3.12)$$

and by introducing Eqs. (3.11) in terms of $U(x,y)$ into the compatibility equation(3.13),

$$\frac{\partial^2 \varepsilon_x}{\partial y^2} + \frac{\partial^2 \varepsilon_y}{\partial x^2} = \frac{\partial^2 \gamma_{xy}}{\partial x \partial y} \quad \ldots (3.13)$$

we get the following biharmonic equation:

$$a_{22}\frac{\partial^4 U}{\partial x^4} - 2a_{16}\frac{\partial^4 U}{\partial x^3 \partial y} + (2a_{12}+a_{66})\frac{\partial^4 U}{\partial x^2 \partial y^2} - 2a_{16}\frac{\partial^4 U}{\partial x \partial y^3} + a_{11}\frac{\partial^4 U}{\partial y^4} = 0 \quad \ldots (3.14)$$

The general solution of Eq.(3.14) depends on the roots of the characteristic equation

$$a_{11}s^4 - 2a_{16}s^3 + (2a_{12}+a_{66})s^2 - 2a_{26}s + a_{22} = 0 \quad \ldots (3.15)$$

and
$$s_1 = \alpha_1 + i\beta_1 \qquad s_2 = \alpha_2 + i\beta_2$$
$$s_3 = \alpha_1 - i\beta_1 \qquad s_4 = \alpha_2 - i\beta_2 \quad \ldots (3.16)$$

The complex parameters given by Eqs.(3.16) depend on the coefficients a_{ij} $(i,j = 1,2,6)$ of the anisotropic plate. The coefficients a_{ij} for the unidirectional layers with oriented

fibers and for symmetric laminates with different lay up can be determined using the equations given in Appendix-I.

The Airy's stress function *U (x,y)* in Eqs.(3.16) can be represented by

$$U(x,y) = F_1(x+s_1y) + F_2(x+s_2y) + F_3(x+s_3y) + F_4(x+s_4y) \quad \ldots (3.17)$$

Or

$$U(x,y) = F_1(z_1) + F_2(z_2) + \overline{F_1(z_1)} + \overline{F_2(z_2)} \quad \ldots (3.18)$$

Introducing the analytic functions $\phi(z_1), \psi(z_2)$ and their conjugates $\overline{\phi(z_1)}$, $\overline{\psi(z_2)}$ given by

$$\frac{dF_1}{dz_1} = \phi(z_1); \quad \frac{dF_2}{dz_2} = \psi(z_2)$$
$$\frac{d\overline{F_1}}{d\overline{z_1}} = \overline{\phi(z_1)}; \quad \frac{d\overline{F_2}}{d\overline{z_2}} = \overline{\psi(z_2)} \quad \ldots (3.19)$$

into Eq. (3.18) and then from Eqs.(3.12), the stress components in terms of $\phi(z_1)$, $\psi(z_2)$ are given by

$$\begin{aligned} \sigma_x &= 2\,\mathrm{Re}\left[s_1^2\,\phi'(z_1) + s_2^2\,\psi'(z_2)\right] \\ \sigma_y &= 2\,\mathrm{Re}\left[\,\phi'(z_1) + \psi'(z_2)\,\right] \\ \tau_{xy} &= -2\,\mathrm{Re}\left[\,s_1\,\phi'(z_1) + s_2\,\psi'(z_2)\,\right] \end{aligned} \quad \ldots (3.20)$$

Stress Functions for Hole Problems under Remote Loading

Scheme of Solution

The anisotropic plate containing the hole is subjected to remotely applied tensions $\sigma_{x'}^{\infty} = \lambda\sigma$, $\sigma_{y'}^{\infty} = \sigma$ at the outer edges as shown in Fig. 3.2 (c). The edges of the hole are free from loading. To determine the stresses around the hole, the solution is split into two stages.

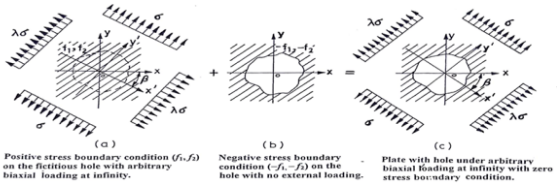

Fig. 3.2 Scheme of Solution for Inplane Loading of Symmetric Laminate with a Hole

First Stage Solution: The stress functions$\phi_1(z_1)$, $\psi_1(z_2)$,are obtained for the hole freeplate due to applied stresses $\sigma_{x'}^{\infty}$, $\sigma_{y'}^{\infty}$ shown in Fig. 3.2(a). The boundary conditions f_1, f_2 on the fictitious hole are determined from these stress functions.

Second Stage Solution: For the second stage solution, the plate with hole is applied by a negative of the boundary conditions f_1, f_2 on its hole boundary in the absence of remote loading as shown in Fig.3.2(b). The stress functions of the second stage solution $\phi_o(z_1)$, $\psi_o(z_2)$ are determined from these boundary conditions.

In accordance with the superposition method of Ukadgaonker and Awasare [34], the stress functions $\phi(z_1)$, $\psi(z_2)$ for the given plate problem are obtained by adding the stress functions of the first and second stage solutions as shown in Fig.3.2(c). They are given by:

$$\phi(z_1) = \phi_1(z_1) + \phi_o(z_1)$$
$$\psi(z_2) = \psi_1(z_2) + \psi_o(z_2) \quad \ldots (3.21)$$

By introducing the above stress functions $\phi(z_1)$, $\psi(z_2)$ into Eqs.(3.20), the stresses σ_x, σ_y, τ_{xy} around the hole are obtained.

RESULTS AND DISCUSSION

Preliminary Remarks

This solution is based on Savin"s [2] approach additionally incorporating the generalized form of mapping function and arbitrary biaxial loading conditions. These features will enhance the simplicity of Savin's method to produce results for any case of hole geometry, laminate material and configuration and type and directions of loading by merely specifying the required combination of parameters. This solution is noted to produce exactly the same results for various cases of solutions existing in the literature.

Computer Implementation of the Solutions

The following steps will help in easy implementation of the given general solutions on the computer.

(a) Choosing the constants of the mapping function, m_k from Table 4.1 for required shape of hole.

(b) Choosing the values of λ and β in Eqs. (3.8)–(3.10) from Section 3.3.2 for type of loading.

(c) Calculation of a_{ij} $(i,j = 1,2,6)$ in Eqs.(3.11) from equations (A.1)–(A.6) given in Appendix-I for single and multilayered plates.

(d) Calculation of complex parameters of anisotropy s_1, s_2 using Eq.(3.15). The values of s_1, s_2 for some selected cases are given in Table 4.2.

(e) Calculation of the constants: a_1, b_1, a_2, b_2, B^*, B'^*, C'^*, K_1, K_2, K_3, K_4, a_3, b_3, a_4, b_4 by using Eqs. (3.7), (3.25), (3.27), (3.31).

(f) Derivatives of the second stage stress functions, $\phi_0'(z_1)$, $\psi_0'(z_2)$ by using Eqs.(3.33).

(g) Evaluation of stresses σ_x, σ_y, τ_{xy} and σ_ρ, σ_θ, $\tau_{\rho\theta}$ by using Eqs.(3.32) and (3.34) respectively.

Table 4.1Mapping function constants

Shape of hole	Mapping function constants
1 Ellipse	$m_1=(a-b)/(a+b)$, a, b are major, minor axes
2 Equilateral Triangle	$m_2=1/3$, $m_6=1/45$, $m_8=1/162$, $m_{11}=7/2673$, $m_{14}=1/729$, $m_{17}=91/111537$
3 Square with	
(a) Normal sides	$m_2=-1/6$, $m_7=1/56$, $m_{11}=-1/176$, $m_{15}=1/384$, $m_{19}=-7/4864$
(b) Rotated by 45°	$m_2=-1/6$, $m_7=1/56$, $m_{11}=-1/176$, $m_{15}=1/384$, $m_{19}=-7/4864$
3 Rectangle	
(a) side ratio:10	$m_1=0.789$, $m_2=-0.0627$, $m_6=-0.0297$, $m_7=-0.014$ $m_9=-0.000564$, $m_{11}=-0.000937$
(b) side ratio: 6	$m_1=0.6813$, $m_2=-0.0893$, $m_6=-0.0365$, $m_7=-0.126$ $m_9=-0.001266$, m11 = 0.00296
(c) side ratio: 5	$m_1=0.643$, $m_2=-0.098$, $m_6=-0.038$, $m_7=-0.011$, $m_9=0.00056$, $m_{11}=0.004$
(d) side ratio: 3.2	$m_1=1/2$, $m_2=-1/8$, $m_6=-3/80$, $m_7=-8/896$, $m_9=5/768$, $m_{11}=57/11264$
4 Other shapes	
i. Circular shape	All constants are zero
ii. Irregular shape	$m_2=0.06$, $m_6=0.04$, $m_7=0.04$
iii. Parabolic shape	$m_2=-0.2$, $m_7=-0.1$
iv. Distorted shape	$m_2=-0.15$, $m_7=-0.07$
v. Distorted shape	$m_2=-0.2$, $m_6=-0.1$
vi. Elliptical shape	$m_1=0.5$
vii. Maize shape	$m_1=0.5$, $m_2=0.1$
viii. Eye shape	$m_1=0.5$, $m_2=0.1$
ix. Bat shape	$m_2=-0.1$, $m_4=-0.15$, $m_5=0.02$, $m_6=-0.05$, $m_7=-0.05$ $m_8=0.02$, $m_9=-0.05$

Table 4.2 : Complex parameters s_1, s_2 for various cases of anisotropy under inplane loading

Fiber Orientation Angle α	*Graphite/ epoxy* E_1(GPa) : 181.00 E_2 (GPa) : 10.30 G_{12} (GPa) : 7.17 ν_{12} : 0.28 ν_{21} : 0.02	*Boron/epoxy* 282.8 23.8 10.35 0.27 0.023	*CP/T300* 63.80 63.80 3.20 0.036 0.036	*Plywood* 11.29 5.89 0.69 0.07 0.134	*Glass/Epoxy* 47.40 16.20 7.00 0.26 0.089
0°	s_1 4.8939i s_2 0.8566i	5.1325i 0.6717i	4.4514i 0.2246i	4.1020i 0.3449i	2.3962i 0.7139i
15°	s_1 -2.2612+1.9287i s_2 0.0677+0.8722i	-2.3486+1.9026i 0.1425+0.6973i	-2.0810+1.9693i 0.2535+0.2399I	-1.9205+1.9911i 0.2341+0.3665i	-0.8997+1.8186i 0.1268+0.7381i
30°	s_1 -1.4750+0.7263i s_2 0.1235+0.9177i	-1.4959+0.6997i 0.2755+0.7785i	-1.4284+0.7804i 0.5391+0.2946I	-1.3826+0.8276i 0.4893+0.4423i	-0.9395+1.0964i 0.2420+0.8137i
45°	s_1 0.1536+0.9814i s_2 -0.9198+0.3923i	0.3782+0.9257i -0.9269+0.3754i	-0.9039+0.4277i 0.9039+0.4277i	0.5007+0.8656i 0.6011+0.7992i	-0.70340+0.7108i 0.3249+0.9458i
60°	s_1 0.1440+1.0703i s_2 -0.5456+0.2687i	0.4039+1.1416i -0.5485+0.2565i	1.4284+0.7804i -0.5391+0.2946i	1.1246+1.0168i –0.5325+0.3187i	0.3359+1.1292i -0.4506+0.5259i
75°	s_1 0.0886+1.1397i s_2 -0.2560+0.2184i	0.2812+1.3766i -0.2571+0.2083i	2.0810+1.9693i -0.2535+0.2399i	1.2375+1.9379i –0.2510+0.2602i	0.2260+1.3160i -0.2186+0.4418i
90°	s_1 0.0000+1.1674i s_2 0.0000+0.2043i	0.0000+1.4888i 0.0000+0.1948i	4.4514i 0.2246i	2.8993i –0.2438i	1.4009i 0.4173i
(±45°),	s_1 -0.8597+0.5109i s_2 0.8597+0.5109i	-0.8891+0.4578i 0.8891+0.4578i	-0.9005+0.4350i 0.9005+0.4350i	-0.8534+0.5213i 0.8534+0.5213i	-0.7966+0.6046i 0.7966+0.6046i
(0°/90°),	s_1 3.6404i s_2 0.2747i	4.1266i 0.2423i	4.3694i 0.2289i	0.3555i 0.2813i	2.0143i 0.4964i

Comparison with existing Results

Results are obtained for laminates without piezo-layers for different shapes of holes in anisotropic plates under in-plane loading. for comparing with those in the literature. Selected cases are presented in the following for brevity.

Lekhnitskii [1]

Lekhnitskii [1] has given the results for a circular hole in plywood plate under X-axis loading, Y-axis loading,

International Journal of Research
Available at https://edupediapublications.org/journals
e-ISSN: 2348-6848
p-ISSN: 2348-795X
Volume 05 Issue-01
January 2018

equi-biaxial and shear loading as given in page No (177) and (181) of Ref.[1].

- Uni-axial tension σ in *x*-axis with E_1 along *x*-axis, the values of σ_θ are given in Fig.80 [1]; the maximum value of σ_ψ is 5.45 at 90^0. Results obtained by the present solution are shown in fig. 4.19 (a) and those obtained by Lekhnitskii [1] are presented in Fig. 4.19 (b). These results are reproduced by ANSYS. As shown in Fig. 4.20.
- Uni-axial tension σ in *x*-axis with E_1 along *y*-axis, the values of σ_θ are given in Fig.81 [1]; the maximum value of σ_θ is 4.15 at 90^0.
- Equi-biaxial tension σ; the stress concentration around hole given in Fig.82 [4] the values of σ_θ are given in Fig.80 [1]; the maximum value of σ_θ is 4.04.
- Shear loading; the stress concentration around hole is given in Fig.86 [1]. The maximum value of σ_θ is 3.95 at 75^0, 105^0, 255^0, 285^0. The results by the present solution are as shown in Fig. 4.11(a) and those by Lekhnitskii [1] are shown in Fig 4.11 (b). The same results are also reproduced by ANSYS as shown in Fig. 4.12.

Results by the present solution for all the above cases are in good agreement with those of Lekhnitskii [1].

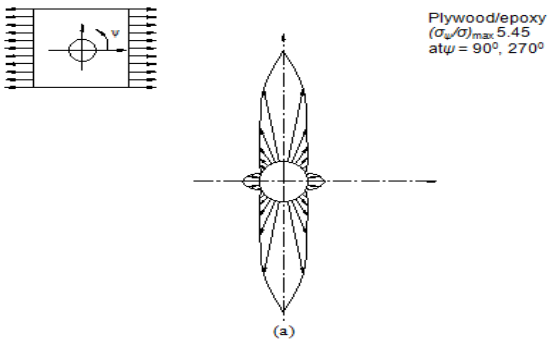

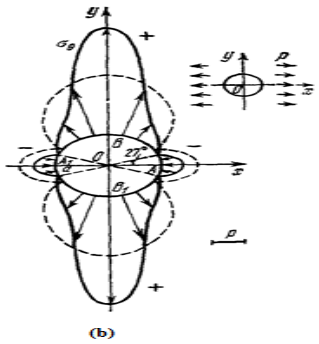

Fig.4.1 Results of Lekhnitskii for circular hole in single layered Plywood /epoxy plate
(a)Present solution (b) Results of Lekhnitskii [1]

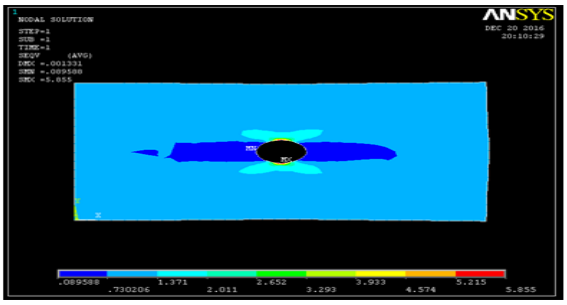

Fig.4.2 ANSYS Results of Lekhnitskii for circular hole in single layered graphite/epoxy plate subjected to X-axis loading.

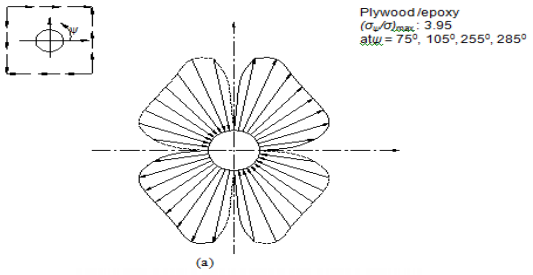

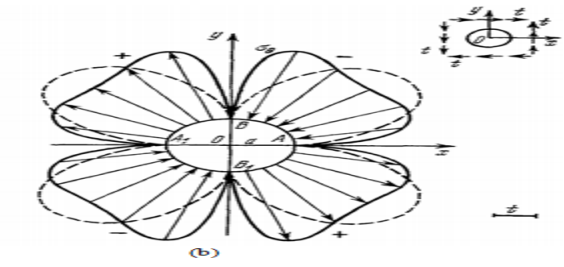

International Journal of Research
Available at https://edupediapublications.org/journals
e-ISSN: 2348-6848
p-ISSN: 2348-795X
Volume 05 Issue-01
January 2018

Fig.4.3 Results of Lekhnitskii for circular hole in single layered Plywood /epoxy plate under shear loading (a) Present solution (b) Results of Lekhnitskii[3]

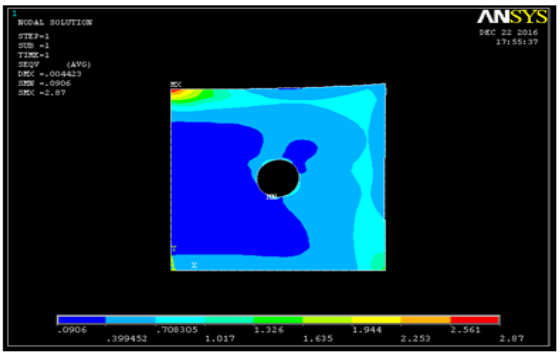

Fig.4.4 ANSYS Results of Lekhnitskii for circular hole in single layered Plywood /epoxy plate under shear loading

Savin [2]

Savin [2] has given results for different shapes of holes in isotropic plate. The present general solution by Stroh formalism given for anisotropic case can be degenerated to isotropic case by taking the corresponding constants as E_1= E_2=E and G_{12}-=G and $\nu_{12} = \nu$. The values of $\sigma_\psi/\sigma$are obtained for the following cases corresponding to the results given by Savin [2].

a) Square hole, mapping function with two and three terms; loading angles 0^0.45^0 the results are given in Table 1[2]
b) Square hole, mapping function with four terms and loading angle; 90^0, the results are given in Table 2[2]
c) Rectangular hole of side ratio 5 and mapping function with 5 terms; loading angles 0^0,30^0, 60^0, 90^0, the results are given in Table 3[2]
d) Rectangular hole of side ratio 3.2 and mapping function with 4 terms; loading angles 0^0, 90^0, the results are given in Table 4[2]
e) Triangular hole given by mapping function with two and three terms; loading angle 0^0; the results are given Table 5[2]
f) Elliptical hole with axes ratios 3/2 and 2/3; loading angle 90^0, the results are given in Table 6 [2]

For all the cases mentioned above, satisfactory results are obtained. For items (c), d) and (e), the results obtained by the present solution and those given by Savin [2] are shown for comparison in Tables 4.3 and 4.6.

Table 4.3: Stress distribution around elliptical hole due to tension along *x*-axis

	Axes ratio b/a =2/3		Axes ratio b/a = 3/2	
Angle	Savin [2]	Present solution	Savin [2]	Present solution
0	-1	-1	-1	-1
10	-0.78	-0.7815	-0.93	-0.9317
20	-0.23	-0.2338	-0.72	-0.7214
30	0.43	0.4282	-0.35	-0.3539
40	1.04	1.0419	0.19	0.1923
50	1.54	1.5373	0.93	0.934
60	1.9	1.9025	1.86	1.8547
70	2.15	2.1484	2.85	2.8497
80	2.29	2.2893	3.67	3.6744
90	2.33	2.3351	4	4.0039

Table 4.4: Results of Savin for various side ratio of Rectangular hole

	Rectangle side ratio:5		Rectangle side ratio:3		Triangle	
Angle	Savin[2]	Present	Savin[2]	Present	Savin[2]	Present
0	-0.768	-1	-0.77	-1	-1	-1
20	-0.152	-0.3848	-0.807	-1.0555	-0.042	-0.0372
25	2.692	2.904	-0.686	-0.9873	0.222	0.2214
30	2.812	3.1353	2.61	2.6888	0.492	0.4908
35	--	--	3.181	3.4595	--	0.5376
40	1.558	-1.7249	2.392	2.6539	--	0.5815
90	1.192	1.1932	1.342	1.3708	1.77	1.7671

Greszczuk [3]

Greszczuk [3] considered a circular hole in unidirectional layers with different fiber orientations as well as bidirectional cross ply and angle ply laminates of Boron /epoxy. The present solution has exactly reproduced the results of Greszczuk for various cases.

a) Boron /epoxy with circular hole for unidirectional layers with 0^0 and 90^0 fibers subjected to shear stress at infinity given in Fig .5 [3].

b) Unidirectional layer of Boron /epoxy with different fiber orientations such as 0^0, 30^0,60^0 and 90^0 fibers, the results are given in Fig.7[[3].

The results reproduced by the present solution are presented in Fig. 4.23 (a) and those given by Greszczuk [3] are presented in Fig. 4.23 (b). These two results are in excellent agreement with each other.

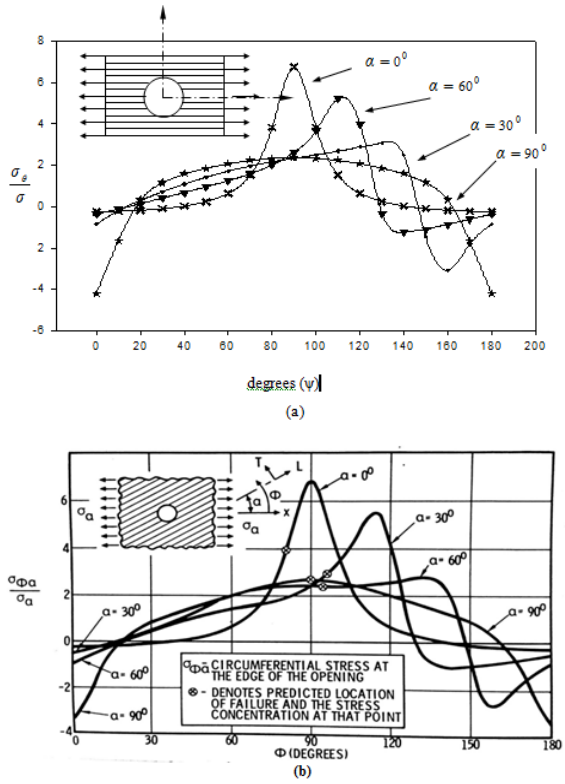

Fig.4.5 Results showing the stresses around circular hole in Boron/epoxy laminate

(a) Present Solution (b) Greszczuk [3]

Jong [5]

Jong [5] considered circular, square and rectangular holes in CFRP laminates subjected to uni-axial loading and shear stress at infinity. The present general solution by Stroh formalism has exactly reproduced for all cases presented by Jong as mentioned below.

a) Square and circular holes in $[0_4/\pm45_4]_s$ and $[\pm45]_s$ laminates subjected to tension in x- direction; the values of σ_θ/σ are given in Table 10[5],

b) Square and rectangular hole in $[\pm45]_s$ laminates subjected to shear stress at infinity, the values of σ_θ/σ are given in Table 14 [5],

The results from the present solution and corresponding to those of Table 9 [5]of Jong are given in Table 4.5 for comparison.

Table 4.5 Results of Jong for circular hole in CFRP laminate under x-axis loading

Angle	Present Solution	Jong:Table 9[5]
0	-1	-1
5	-0.9968	-0.9967
10	-0.9843	-0.9842
15	-0.9531	-0.9531
20	-0.8832	-0.8831
25	-0.7362	-0.7362
30	-0.4469	-0.4468
35	0.0726	0.0726
40	0.8636	0.8636
45	1.7742	1.7741
50	2.469	2.4689
55	2.7634	2.7633
60	2.7556	2.7556
65	2.6163	2.6163
70	2.453	2.453
75	2.3122	2.3122
80	2.2093	2.2093
85	2.1477	2.1477
90	2.1273	2.1273

Daoust and Hoa [6]

Daoust and Hoa [6] has obtained the stresses around an equilateral triangular hole for various cases. The present general solution has exactly reproduced all the results. Some of the cases are presented below.

a) Triangular hole with 4 terms of mapping function in a glass epoxy lamina with 0^0 fiber, ε = ½ ; the stresses σ_θ/σ are given in Table 4.4 [6].

b) For different values of ε i.e., ε = 1/3, 1/6,1/8 , 0 (circle), with 4 terms mapping function; the values of σ_θ/σ are given in Fig. 4.5 [6]

c) Unidirectional layers with 0^0 fibers of different materials viz., Graphite/epoxy, plywood, Glass/epoxy and isotropic case under uni-axial tension; the maximum values of σ_θ/σ are shown in Fig.4.6 [6].

The results have obtained corresponding to item (c) above, by the present solution are given in Fig.4.24 and Table 4.8. The results by the present solution are good agreement with those of Daust and Hoa[6].

Table 4.6: Results of Daoust &Hoa [6]

Angle	Present solution	Daoust & Hoa [6]
0	-0.5846	-0.167
10	-0.1795	-0.167
20	0.0491	0.063
30	0.1651	0.178
40	0.245	0.258
50	0.3209	0.334
60	0.4114	0.426
70	0.5373	0.554
80	0.7373	0.756
90	1.1107	1.132
100	2.019	2.039
110	5.9073	5.879
115	12.1251	12.131
120	6.2503	6.278
130	0.0251	0.053
140	-0.6088	-0.643
150	-0.6417	-0.679
160	-0.6146	-0.649
170	-0.5924	-0.625
180	-0.5846	-0.617

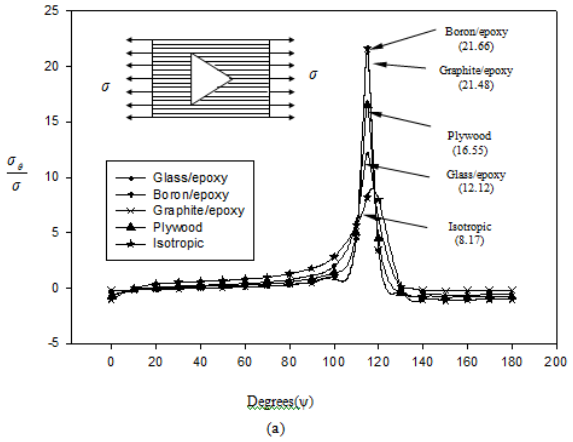

(a)

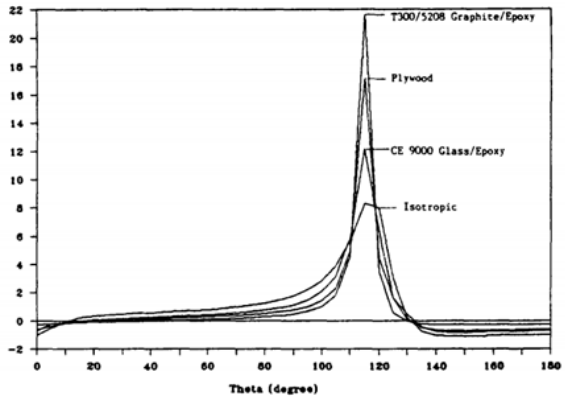

(b)

Fig.4.6 Results showing the effect material on stress distribution around triangular hole

(a) Present solution (b) Daoust and Hoa [6]

Results for New Cases

To illustrate the effectiveness and scope of the present solution, results for several new cases of laminates containing different shapes of holes and loading conditions are presented in this section. Circular, elliptical, arbitrary isosceles triangular hole [6], rectangular hole with different side ratios, square hole and holes of irregular geometry are considered. A detailed study is presented on the effect of shape of hole, type of material, fiber orientation, laminate geometry, type and angle of loading on stress distribution around the hole.

Effect of Material

International Journal of Research
Available at https://edupediapublications.org/journals
e-ISSN: 2348-6848
p-ISSN: 2348-795X
Volume 05 Issue-01
January 2018

Stress concentration is very much influenced by the material properties and has a detrimental effect especially in case of anisotropic materials. A triangular hole is considered in single layered plates of graphite/epoxy and glass/epoxy, Boron/epoxy, plywood, CF and Isotropic materials under equi-biaxial loading. For graphite/epoxy, it is equal to 28.14 and for glass/epoxy, it is 32.39 at 0^0. The maximum value of stress for Boron/epoxy, plywood, CF and isotropic materials is equal to 29.37, 53.80, 78.28 and 34.09 at 120^0 respectively. In all the cases, the maximum value has occurred at the corners only as shown in Fig. 4.28.

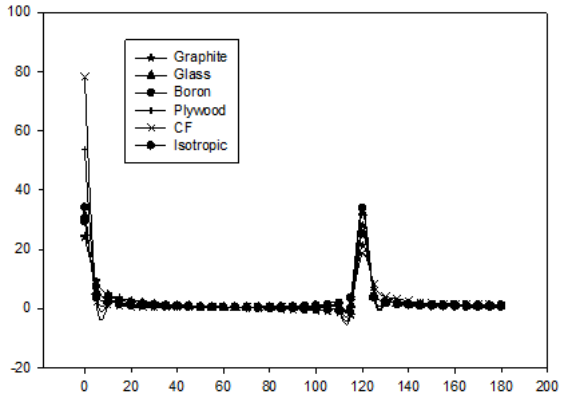

Fig.4.7 Effect of material on stress around triangular hole due to equi-biaxial loading

Effect of Fiber Orientation

Anisotropy of the lamina is influenced by the fiber orientation. Different fiber orientations such as 0^o, 30^o, 45^o, 60^o and 90^o are considered in a lamina of graphite/epoxy with triangular hole under X-axis loading. The results for all fiber angles are presented in Fig. 4.29. For fiber orientation angle, $\alpha = 0^0$ the maximum stress is equal to 11.62 and a nearest result has occurred by ANSYS as shown in Fig.4.30. For fiber angle, $\alpha = 30^0$, the maximum value of σ_θ/σ is equal to 77.3 as shown in Fig.4.31. Results by ANSYS for 45^0, 60^0 and 90^o are shown in Figs. 4.32 to 4.34.

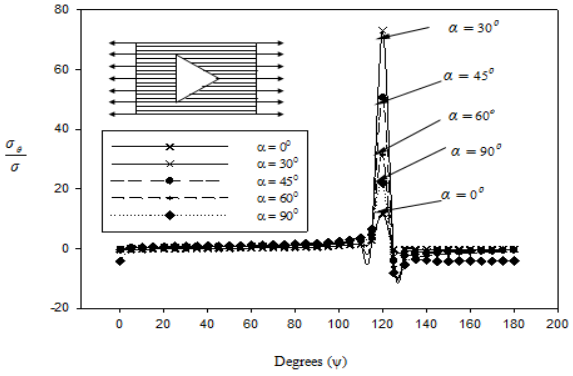

Fig 4.8 Effect of fiber orientation on stress around triangular hole in Graphite/epoxy plate

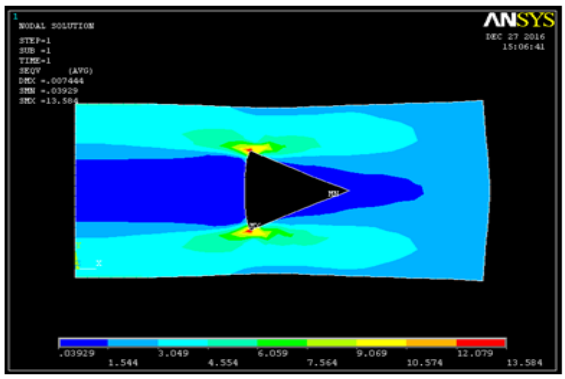

Fig 4.9 ANSYS Result showing the Effect of fiber orientation at 0^0on stress distribution around triangular hole in Graphite/epoxy plates subjected to X-axis loading

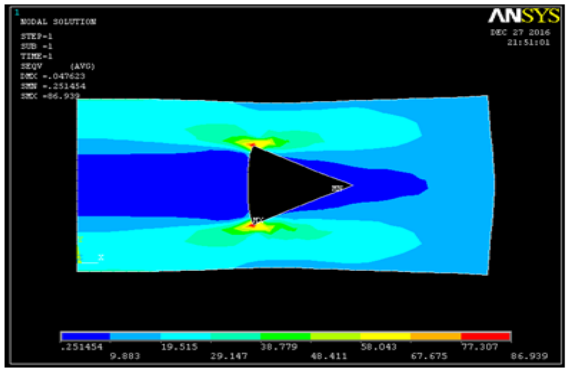

Fig 4.10 ANSYS result showing the effect of fiber orientation at 30^0on stress distribution around triangular hole in Graphite/epoxy plate subjected to X-axis loading

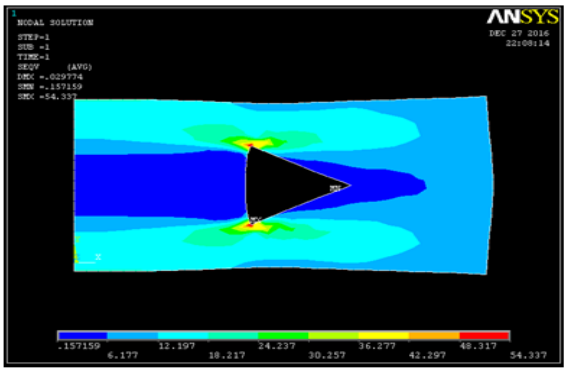

Fig 4.11 ANSYS result showing the Effect of fiber orientation at 45^0on stress distribution around triangular hole in Graphite/epoxy plate subjected to X-axis loading

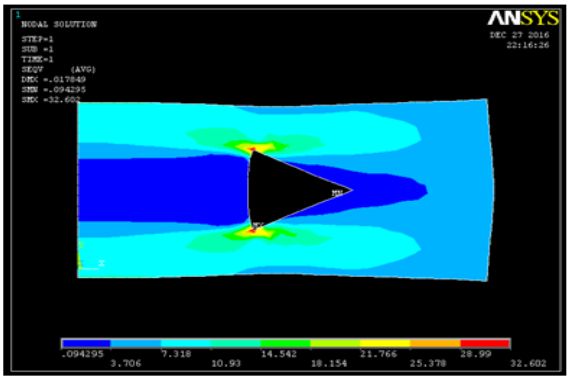

Fig 4.12 ANSYS Result showing the Effect of fiber orientation at 60^0on stress distribution around triangular hole in Graphite/epoxy plate subjected to X-axis loading

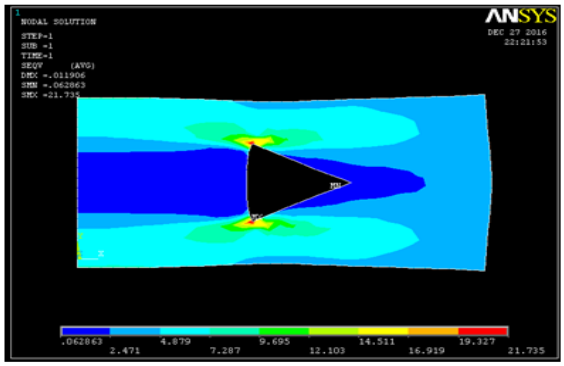

Fig 4.13 ANSYS Result showing the effect of fiber orientation at 90^0on stress distribution around triangular hole in Graphite/epoxy plate subjected to X-axis loading

Effect of Laminate Geometry

Anisotropy of the composite laminates is dependent on fiber orientation and stacking sequence. Graphite/epoxy laminates with different stacking sequences of $[0/90]_s$, $[30/0/-30]_s$and $[45/-45]_s$ around square and triangular holes subjected to X-axis loading are considered. The maximum stress concentration around square hole for $[0/90]_s$, $[30/0/-30]_s$ and $[45/-45]_s$ laminates is equal to 7.85, 5.73 and 13.95 respectively. For $[0/90]_s$, $[30/0/-30]_s$ laminates, the maximum stress concentration has occurred at 50^0 whereas for $[45/-45]_s$ laminate, the maximum value is at 45^0. The results for different laminates with square hole are presented in Fig. 4.35. The maximum stress value for triangular hole in $[0/90]_s$, $[30/0/-30]_s$ and $[45/-45]_s$ laminates, is equal to 16.16, 25.83 and 30.39 respectively at 120^0. Weak zone has occurred at 45^0 for $[45/-45]_s$ laminate with a square hole and it is occurring at 120^0 for all geometries with a triangular hole. The results for different laminates with a triangular hole are presented in Fig. 4.36. The laminate geometry, fiber orientation and shape of hole have a combined effect on the maximum value of stress concentration.

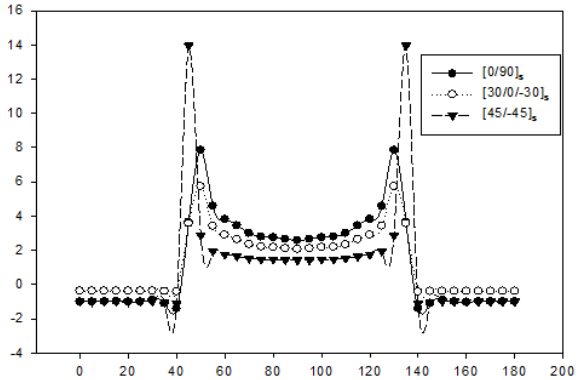

Fig. 4.14 Effect of Laminate geometry on stress distribution around square hole

Effect of Type of Loading

Type of loading has a great influence on the stress distribution around the hole. Different types of loading such as X-axis, Y-axis, equi-biaxial and shear loadings are

International Journal of Research
Available at https://edupediapublications.org/journals
e-ISSN: 2348-6848
p-ISSN: 2348-795X
Volume 05 Issue-01
January 2018

considered on a Graphite/epoxy unidirectional lamina with a triangular hole. The results for these cases are presented in Fig.4.37. The maximum values of σ_θ/σ for X-axis loading is equal to 11.62, for Y-axis loading is equal to 16.51, for equi-biaxial loading, it is equal to 28.17 and for shear loading it is 37.27. The stress concentration is maximum for shear loading and minimum for X-axis loading.

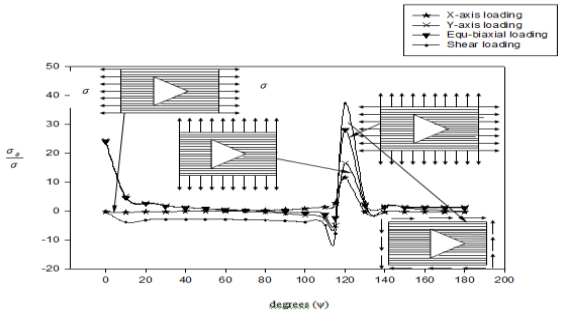

Fig. 4.16 Effect of type of loading on stress distribution around triangular hole in Graphite/epoxy plates

Effect of Angle of Loading

The influence of angle of loading β on stress distribution around the hole is studied for different angles of loading from 0^0 to 90^0 on a cross ply laminate of graphite/epoxy with rotated square hole. Different angles of loading from 0^0 to 90^0 with intervals of 15^o are considered and the maximum values of stress concentration are 28.90, 26.89, 21.42, 13.95, 21.42, 26.89 and 28.90 for each corresponding angle of loading. These results are presented in Fig. 4.38. It is that for loading angles between 0^0 to 45^0, the maximum stress concentration has occurred at 90^0 and for loading angles between 45^0 to 90^0, the maximum value has occurred at 0^0. From this study, we can infer that the stress concentration can be controlled by proper combination fiber orientation and angle of loading.

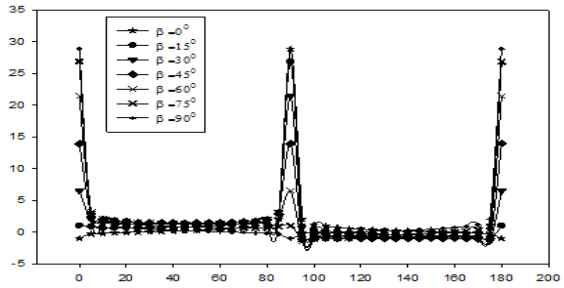

Fig.4.17 Effect of angle of loading on stress distribution around rectangular hole in $[0/90]_s$ graphite/epoxy laminate

Effect of Shape of Hole

Stresses distribution around the holes in a laminates depends on the shape of hole, which in turn is affected by the number of terms in the mapping function, bluntness factor and side ratio or aspect ratio, etc. In the present study, different shapes of holes, such as, circle, ellipse, triangle, square, rectangular hole with various side ratios, pentagon, hexagon, heptagon and octagon are considered in graphite/epoxy cross play laminate $[0/90]_s$ subjected to X-axis loading. For all these cases, results by ANSYS software are also presented for comparison.

Circular Hole

The stress distribution around circular hole in $[0/90]_s$ laminates of graphite/epoxy and Boron/epoxy under uni-axial tension is presented in Fig. 4.39 and Fig. 4.40 respectively. For graphite/epoxy, the maximum value of σ_θ/σ is 4.9 and for boron/epoxy, it is 5.1. The maximum value has occurred at 90^o for both cases.

Results by ANSYS software are also presented in Figs. 4.41 and 4.42 respectively. The maximum value of von-Mises stress for graphite/epoxy is equal to 5.29 and it is equal to 5.25 for born/epoxy. These results show good agreement with the results from the general solution.

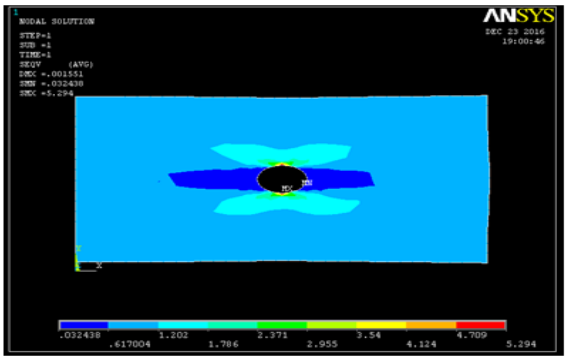

Fig. 4.20 ANSYS results for Stress distribution around circular hole in $[0/90]_s$ Graphite/epoxy laminate subjected to X-axis load.

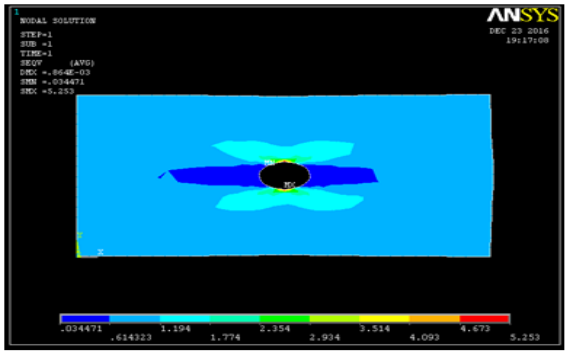

Fig. 4.21 ANSYS results for stress distribution around circular hole in $[0/90]_s$ Boron/ epoxy laminate subjected to X-axis loading.

Elliptical hole

The value of σ_ψ/σaround the elliptical hole in $[0/90]_s$ laminates of Graphite/epoxy and Boron/epoxy under uni-axial tension is presented in Fig.4.43 and Fig.4.44 respectively. The maximum value of $\sigma_\theta/\sigma$is equal to 2.96 for Graphite/epoxy and 3.05 for Boron/epoxy. The maximum value of stress σ_ψ/σhas occurred at 90° in both cases.

Results are obtained by ANSYS for both the above cases are shown in Figs. 4.45 and 4.46 respectively. The maximum value of von-Mises stress for graphite/ epoxy is equal to 2.89 whereas, for boron epoxy, it is equal to 2.87. The results by the general solution are in good agreement with those obtained by ANSYS.

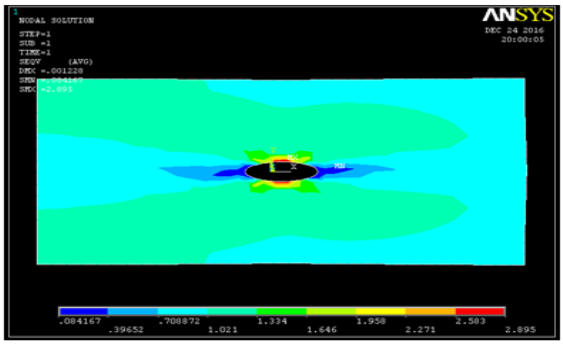

Fig. 4.24ANSYS results for Stress distribution around elliptical hole in $[0/90]_s$ Graphite/epoxy laminate subjected to X-axis loading

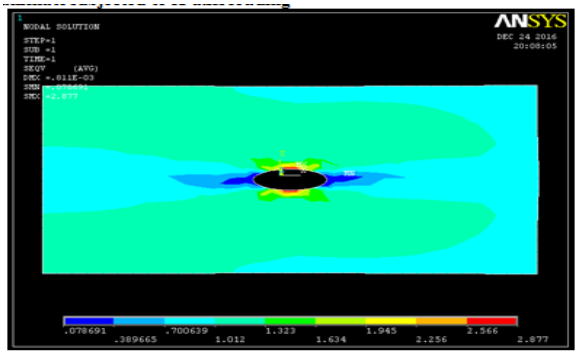

Fig. 4.25 ANSYS results for Stress distribution around elliptical hole in $[0/90]_s$ Boron/epoxy laminate subjected to X-axis loading.

Triangular Hole

The stress distribution around triangular hole in $[0/90]_s$ laminates of Graphite/epoxy and Boron/epoxy under X-axis loading is shown in Fig.4.47 and 4.48 respectively. For Graphite/epoxy, the maximum value of $\sigma_\psi/\sigma$is equal to 16.16 and for Boron/epoxy, it is equal to 15.54. The maximum value of σ_ψ/σ has occurred at 120°and 240° for both cases.

International Journal of Research
Available at https://edupediapublications.org/journals
e-ISSN: 2348-6848
p-ISSN: 2348-795X
Volume 05 Issue-01
January 2018

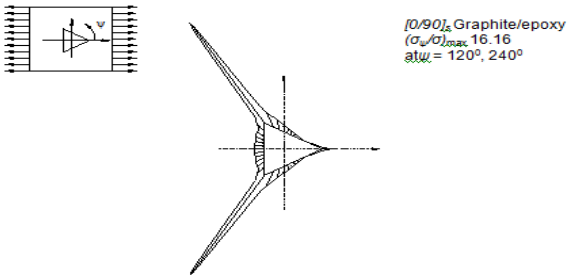

Fig 4.26 Stress distribution around triangular hole in $[0/90]_s$ Graphite/epoxy laminate

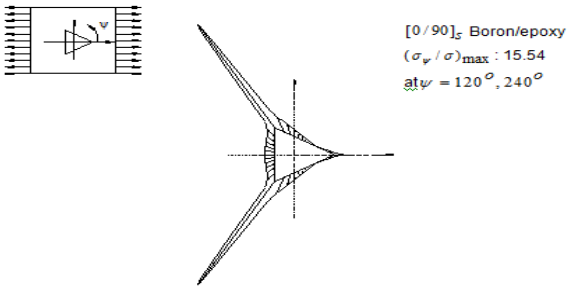

Fig 4.27Stress distribution around triangular hole in $[0/90]_s$ Boron/epoxy laminate

Results obtained by ANSYS for the above cases are shown in Figs. 4.49 and 4.50. For Graphite/epoxy, the maximum values of von-Mises stress is 18.09 and for Boron /epoxy, it is equal to 17.69. These results are very much comparable to those obtained by the general solution.

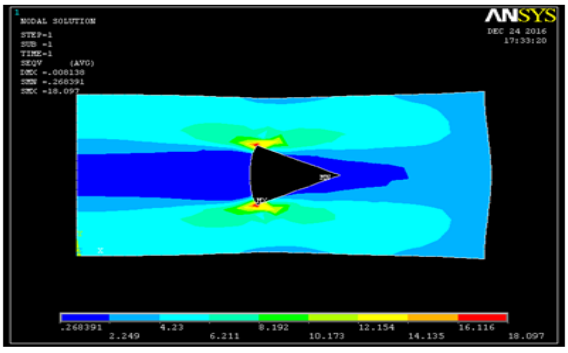

Fig. 4.28 ANSYS results for Stress distribution around triangular hole in $[0/90]_s$ Graphite/epoxy laminate subjected to X-axis loading.

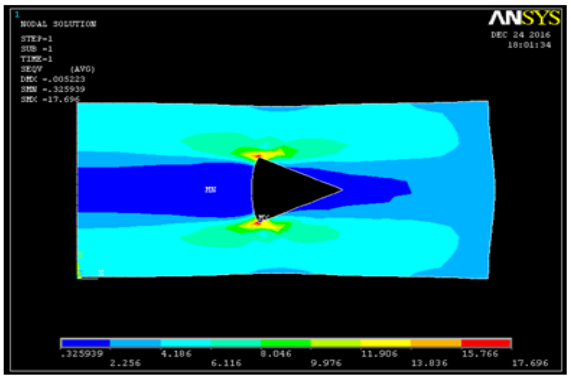

Fig. 4.29ANSYS Results for Stress distribution around triangular hole in $[0/90]_s$ Boron/epoxy laminate subjected to X-axis loading.

Normal Square Hole

The stress distribution around normal square hole in $[0/90]_s$ cross-ply laminate of Graphite/epoxy under x-axis loading is shown in Fig.4.59. The maximum normalized stress σ_ψ/σ is 7.851 at 50^0, 130^0, 230^0, 310^0. The stress distribution for $[45/-45]_s$ cross ply laminate under x- axis loading is also obtained with a maximum value of σ_ψ/σ equal to 13.95 at 45^0, 135^0, 225^0, 315^0. Results for these cases are also presented in Table 4.8 for clarity. Results are obtained by ANSYS for $[0/90]_s$ cross-ply laminate as shown in Fig.4.60 for comparison. It is noted that the results by the present solution have good agreement with those by FEM.

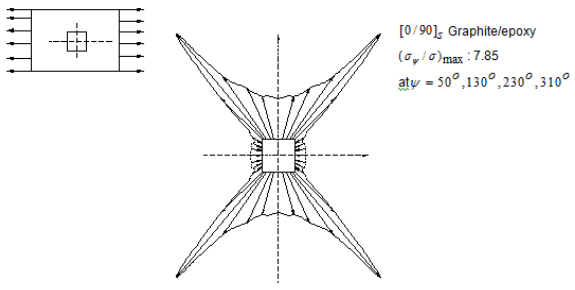

Fig.4.30 Stress distribution around normal square hole in $[0/90]_s$ graphite/epoxy cross ply laminate under X-axis loading

International Journal of Research
Available at https://edupediapublications.org/journals
e-ISSN: 2348-6848
p-ISSN: 2348-795X
Volume 05 Issue-01
January 2018

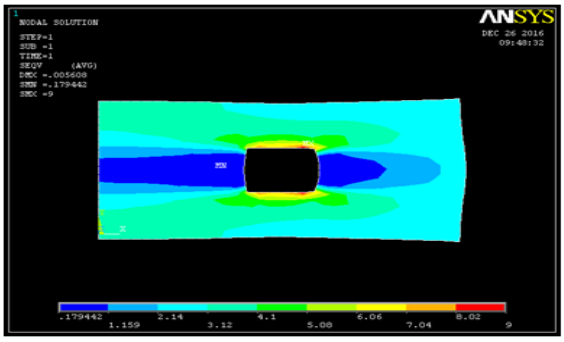

Fig. 4.31 ANSYS results for Stress distribution around square hole with normal side in $[0/90]_s$ Graphite/epoxy laminate subjected to X-axis loading

Rotated Square Hole

The normalized stresses around the rotated square hole in $[0/90]_s$ Graphite/epoxycross-ply laminate are presented in Fig. 4.61. The maximum normalized stress σ_ψ/σ is 28.9 at 90^0. These results are compared with the results by FEM shown in Fig. 4.62 where the maximum value of von-Mises stress is 34.96. Results are also obtained for the rotated square hole in $[45/-45]_s$ angle ply laminate of Graphite/epoxy under X-axis loading and are presented in Table 4.8. The maximum value of σ_ψ/σ is equal to 8.28 at 90^0 itself. In both the cases, the maximum value is occurring at 90°, while it is occurring at 45° and 50° for the normal square hole.

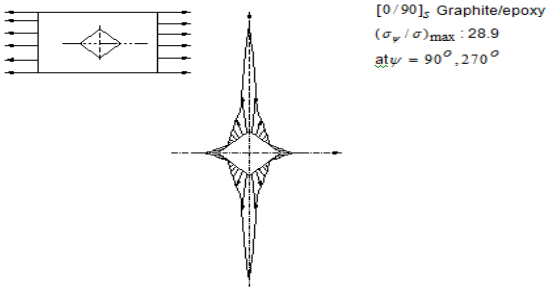

Fig.4.32 Stress distribution around rotated square hole in $[0/90]_s$ graphite/epoxy cross ply laminate under X-axis loading

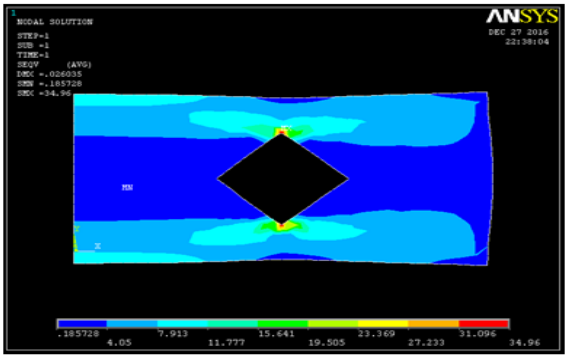

Fig. 4.33 ANSYS result for Stress distribution around rotated square hole in $[0/90]_s$ Graphite/epoxy laminate subjected to X-axis loading

Table. 4.7: Stress distribution around Square holes in graphite/epoxy laminate under *x*-axis loading

Square hole with sides rotated by 45°			Square with normal sides		
Angle	[0/90], cross ply laminate	[45/-45], angle ply laminate	Angle	[0/90], cross ply laminate	[45/-45], cross ply laminate
0	1	-1	0	-1	-1
5	-0.2955	-0.8309	5	-1.0033	-1.0012
10	-0.2209	-0.7324	10	-0.9949	-0.9988
20	-0.0683	-0.2522	20	-1.0225	-1.0064
30	0.0336	0.0919	30	-0.9129	-0.9791
40	0.1538	0.6343	40	-1.4108	-1.1211
45	0.2057	0.7884	45	3.6408	13.9512
50	0.2774	1.0163	50	7.851	2.8576
60	0.4356	1.705	60	3.8122	1.7407
70	0.7042	2.6887	70	2.9963	1.5224
80	1.136	4.2199	80	2.7516	1.4574
85	2.032	7.2711	85	2.6539	1.4323
90	28.9025	8.2816	90	2.5767	1.4115
95	2.032	7.2711	95	2.6539	1.4323
100	1.136	4.2199	100	2.7516	1.4574
105	0.8978	3.5385	105	2.7866	1.4667
110	0.7042	2.6887	110	2.9963	1.5224
120	0.4356	1.705	120	3.8122	1.7407
130	0.2774	1.0163	130	7.851	2.8576
135	0.2057	0.7884	135	3.6408	13.9512
140	0.1538	0.6343	140	-1.4108	-1.1211
150	0.0336	0.0919	150	-0.9129	-0.9791
160	-0.0683	-0.2522	160	-1.0225	-1.0064
170	-0.2209	-0.7324	170	-0.9949	-0.9988
175	-0.2955	-0.8309	175	-1.0033	-1.0012
180	-1	-1	180	-1	-1

Rectangular hole

Different side ratios of rectangular holes such as 3, 5 and 10 are considered to consider the effect of aspect ratio on stress distribution around the rectangular hole. These holes are considered in cross ply laminate $[0//90]_s$ subjected to

International Journal of Research
Available at https://edupediapublications.org/journals
e-ISSN: 2348-6848
p-ISSN: 2348-795X
Volume 05 Issue-01
January 2018

X-axis loading. The results by the general solutions are compared with those obtained by ANSYS.

Side ratio 3

For a rectangular hole with side ratio 3 in a cross ply laminate $[0/90]_s$ of graphite/epoxy, the stress distribution around the hole is shown in Fig.4.34. The maximum value of σ_ψ/σ is 6.16 at 35^0,145^0 .

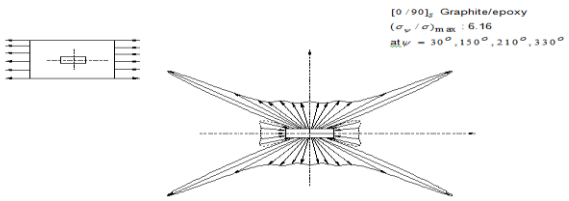

Fig 4.34 Stress distribution around rectangular hole of side ratio 3 in $[0/90]_s$ Graphite/epoxy cross ply laminate subjected to X-axis loading

The above case is also studied by ANSYS and the results are presented in Fig.4.35. The maximum value of von-Mises stress is equal to 6.20. This shows that the results by the general solution are in good agreement with those obtained by ANSYS.

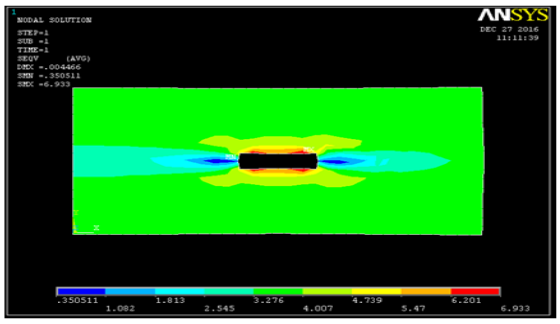

Fig. 4.35 ANSYS results for Stress distribution around rectangular hole of side ratio 3 in $[0/90]_s$ Graphite/epoxy laminate subjected to X-axis loading

Side ratio 5

The stress distribution around the rectangular hole of side ratio 5 in $[0/90]_s$ cross ply laminates of Graphite/epoxy and Boron/epoxy under *x*-axis loading is presented in Fig.4.36 and Fig.4.37 respectively. The maximum value of σ_ψ/σ for graphite/epoxy is equal to 5.37 and for boron /epoxy, it is equal to 5.51. In both the cases, the maximum value of σ_ψ/σhas occurred at 30^o.

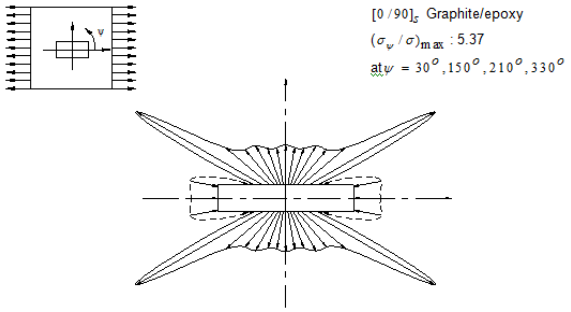

Fig 4.36 Stress distribution around rectangular hole of side ratio 5 in $[0/90]_s$ Graphite/epoxy laminate subjected to X-axis loading

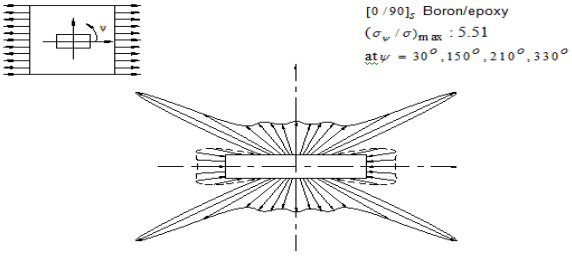

Fig 4.37 Stress distribution around rectangular hole of side ratio 5 in $[0/90]_s$ Boron/epoxy laminate subjected to X-axis loading

The results obtained by ANSYS for the above cases are shown in Fig.4.38 and 4.39. The maximum values of von-Mises stress forgraphite/epoxy is 6.7 and for boron /epoxy, it is equalto 6.56. These results show good agreement withthose by the general solution.

International Journal of Research
Available at https://edupediapublications.org/journals
e-ISSN: 2348-6848
p-ISSN: 2348-795X
Volume 05 Issue-01
January 2018

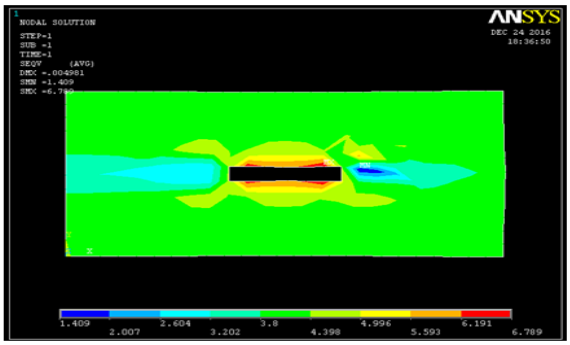

Fig.4.38 ANSYS results for Stress distribution around rectangular hole of side ratio 5 of Graphite/epoxy $[0/90]_s$ subjected to X-axis loading

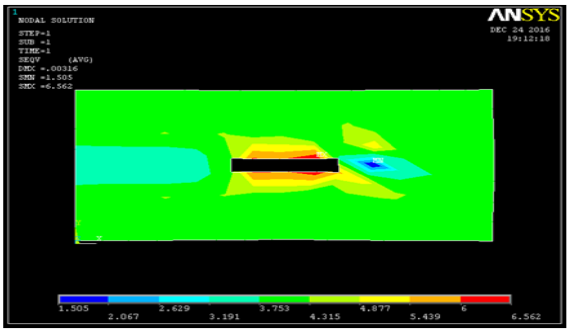

Fig.4.39 ANSYS Result for Stress distribution around rectangular hole of side ratio 5 in $[0/90]_s$ Boron/epoxy laminate subjected to X-axis loading

Side Ratio 10

The stress distribution around rectangular hole of side ratio 10 in $[0/90]_s$ cross ply laminate of graphite/epoxy under X-axis loading is shown in Fig.4.40. The maximum value ofσ_ψ/σ by the general solution is 3.66 at 25^0,155^0 and it is equal to 4.12 by ANSYS as shown in Fig. 4.41. Results by both the cases have good agreement.

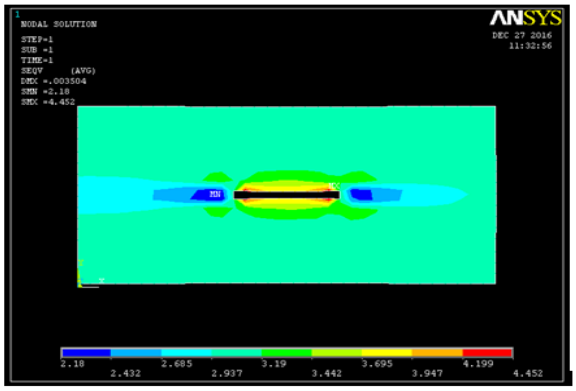

Fig. 4.41 ANSYS Results for stress distribution around rectangular hole of side ratio 10 in $[0/90]_s$ Graphite/epoxy laminate subjected to X-axis loading

Conclusions

- Consideration of the generalized form of mapping function and the arbitrary biaxial loading condition into the boundary conditions has facilitated the derivation of general solutions out of the existing formulations.
- The influence of various parameters viz., hole shape, fiber orientation, laminate geometry, stacking sequence and type of loading, etc., on distribution of stresses or moments around the hole can be studied.
- The constants provided for the mapping functions of various shapes of holes and the complex parameters of anisotropy for inplane loading on symmetric laminates.
- The solution for inplane loading has given satisfactory results for both anisotropic and isotropic cases.
- Various irregular shaped holes are considered for each category of loading.

General Remarks

Based on the results obtained from the general solutions, the following remarks are made.

- Solution for any ratio of biaxial stresses or moments and shear stress or twisting moment can be obtained without the need for superposition of the solutions of uniaxial loading.
- Proper fiber orientation and angle of loading will considerably reduce the maximum stress around the hole.
- In case of a rectangular hole, the locations of maximum stress occur away from the corners. However, these locations and values depend on the aspect ratio of the hole, corner radius and type of loading.
- Critical locations of failure obtained by failure criteria do not coincide with the locations of maximum stress concentration. This feature is in confirmation with the results given in the literature.
- For symmetry of hole shape and loading about the coordinate axes, the stress distributions are symmetric under inplane loading in both isotropic and anisotropic cases. The distributions of moments are not symmetric either due to bending or due to the effect of bending extension coupling in anisotropic case.
- The stress distribution is uniform for all ply groups in a laminate under inplane loading.

Limitations

- Consideration of any new shape of hole, other than those given in the present work, requires its mapping function.
- The equations of present solutions are retained in parametric form due to the large number of parameters involved.

Suggestions for Future Work

- The solution can be extended to consider hygro-thermal stresses.

REFERENCES

[1] Lekhnitskii, S.G., *Anisotropic Plates*, Gordon and Breach, New York, 1968.

[2] Savin, G.N., *Stress Concentration around Holes*, Pergamon Press, New York, 1961.

[3] Greszczuk, L.B., Stress Concentrations and Failure Criteria for Orthotropic and Anisotropic Plates with Circular Openings, *Composite Materials: Testing and Design (Second Conference), ASTM STP 497*, ASTM, 1972, pp. 363-381.

[4] Hayashi, Takaya, Stress Analysis of the Anisotropic Plate with a Hole under the Uniaxial Loading, *Composites '86: Recent Advances in Japan and the United States*, K. Kawata, S. Umekawa and A. Kobayashi, eds, *Proc. Japan, U.S.C.C.M – III*, Tokyo, 1986, pp. 197-204.

[5] Jong, T.D., Stresses around Rectangular Holes in Orthotropic Plates, *Journal of Composite Materials*, 15, 1981, pp. 311-328.

[6] Daoust, J. and Hoa, S.V., An Analytical Solution for Anisotropic Plates Containing Triangular Holes, *Composite Structures*, 19, 1991, pp. 107-130.

[7] Hufenbach, W., Schaffer, M. and Herrmann, A.S., Calculation of the Stress and Displacement Field of Anisotropic Plates with Elliptical Hole, *Ingenieur-Archiv*, 60, 1990, pp. 507-517.

[8] Huffenbach, W. and Kroll, L., Stress Concentration in Notched Anistropically Fiber-Reinforced Plates, *Archive of Applied Mechanics*, 62, 1991, pp. 277-290.

[9] Ukadgaonker, V.G. and Awasare, P.J. A Novel Method of Stress Analysis of Infinite Plate with Circular Hole with Uniform Loading at Infinity, *IndianJournal of Technology*, 31, 1993, pp.539-541.

[10] Ukadgaonker, V.G. and Awasare, P.J. A Novel Method of Stress Analysis of an Infinite Plate with Elliptical Hole with Uniform Tensile Stress, *Journal of the Institution of Engineers (India)*, MC, 73, 1993, pp. 309-311.